

Nanostructured Ti-Mg-Fe Alloy Via Mechanical Alloying Synthesis and Characterization

Dr M Balaji

Assistant Professor,

Rao Bahadur Y. Mahabaleswarappa Engineering College
Ballari, Karnataka, India

Ajeya H

PG Student-MPM

Rao Bahadur Y. Mahabaleswarappa Engineering College
Ballari, Karnataka, India

Abstract—The experimental results of creating and describing the ternary Ti- Mg-Fe alloy are presented in this work. To achieve nanoscale grain refinement, the study employs mechanical alloying through ball milling to synthesize a Ti-Mg-Fe alloy powder with an atomic composition of 60:20:20. Additionally, the creation of ternary Ti- Mg-Fe alloys may enhance their structural qualities while lowering their density, which would make them appropriate for use in biomedical applications. In order to effectively replace a broken bone, orthopaedic implants must have a porous structure that allows human bodily fluids, tissues, and muscles to pass through them. Therefore, it may be possible to make the alloy biodegradable and biocompatible by alloying magnesium with the element sulfur.

The goal of this work was to create a nanostructured ternary titanium-based alloy by alloying it with Mg-Fe because of its favorable biocompatible and biodegradable properties. X-ray diffraction (XRD), scanning electron microscopy (SEM) with EDAX, and high resolution transmission electron microscopy (TEM) were used to characterize mechanically alloyed powders and solid compacts in order to examine structural, phase transformation, compositional, morphological, and topographic factors. Therefore, the mechanically alloyed nanostructured Ti-Mg-Fe alloy may be a promising biomaterial for orthopaedic and dental applications.

I. INTRODUCTION

Ti alloys are amongst the utmost desirable metallic materials in aerospace, biomedical, and engineering sectors, owing to their low density, exceptional strength-to-weight ratio, superior corrosion resistance, and excellent biocompatibility. The demand of micro and nano-devices construction drives the production of new types of alloys as well as their further exploration on different scales. Nevertheless, the nonconventional techniques, including powder metallurgy and concentrated on chemical composition homogeneity, powder morphology and size parameters of the various synthesizing techniques, the present study aims on creating Ti-Mg-Fe alloy powder through powder metallurgy technique.

- **Titanium:** Titanium was found by William Gregor in 1791, a British clergyman, mineralogist and chemist., extracted from the sand (magnetic) of the local stream, Helford, at Menachn Valley, Cornwall, England and separated black sand, presently called as ilmenite. He produced the impure oxide by extracting iron with help of magnet. Later he named it as mechanite. Martin Heinrich Klaproth, a Berlin chemist, extracted TiO₂ from a Hungarian mineral now called as rutile.

- **Magnesium:** Sir Humphrey Davy discovered magnesium as a chemical component in 1808. The difficulty in isolating magnesium was linked to its conductivity, which plagued an interest to use magnesium as a part. In today's material corrosion is considered as one of the key issues. When other properties, such as elastic rigidity, the coefficients are reported to be lower than that of other metals. Germany, and Israel in another. Since 1993, there was a resurgence of interest in Mg alloys for automotive, household, as well as sports equipment's. The weight savings are the driving force.
- **Iron:** Almost all aquatic ecosystems include iron (Fe), the fourth most prevalent element in the Earth's crust. The average amount of iron in sedimentary rocks is between 5 and 6 percent by weight, and the amount of iron engaged in environmental redox processes is about 3.5×10^{12} mol/year. In addition to having direct and indirect effects on corrosion, the breakdown of organic and inorganic compounds, metal mobility, the evolution and sequestration of natural organic matter (NOM), mineral dissolution, nutrient availability, rock weathering and diagenesis, and microbial activity, iron is a key component of the global biogeochemical cycles of many other major and minor elements (such as C, O, N, and S).

II. LITERATURE SURVAY

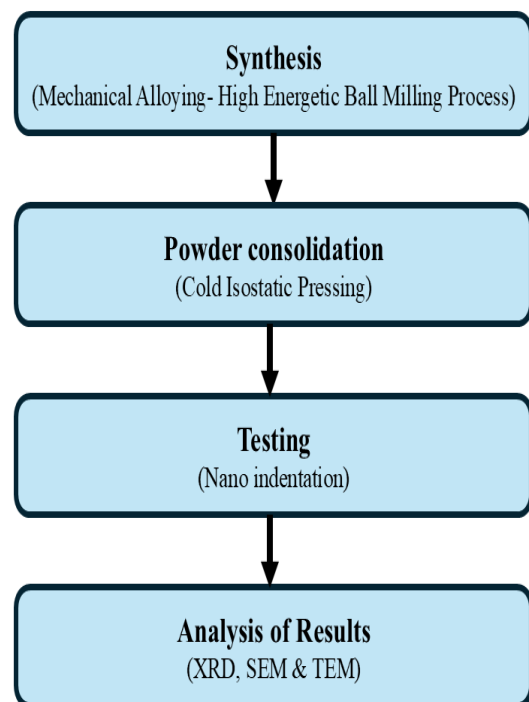
Fatemeh Alijani, et al. [12] The study investigates the influence of the milling process on the chemical composition, microstructure, hardness, and thermal behaviours of Ti-41Ni-9Cu compounds synthesized via mechanical alloying. Structural analysis of the alloyed powders was conducted using X-ray diffraction (XRD), while SEM with EDS was employed to assess chemical homogeneity, particle morphology, and size distribution. Vickers micro-indentation testing was used to evaluate the hardness of powders subjected to varying milling durations. Additionally, differential scanning calorimetry (DSC) was performed to examine the thermal response of the as-milled powders. Results revealed that during the early stages of milling (0–12 hours), the material primarily consisted of a nickel-based solid solution and an amorphous phase. As milling progressed, nanocrystalline martensitic (B19) and austenitic (B2) phases emerged—initially from the raw constituents and subsequently from the amorphous matrix. Continued milling led to improved compositional uniformity, reduced interlayer thickness, and a non-linear trend in micro-hardness: an initial increase followed by a decrease and a subsequent rise. Furthermore, both the thermal behaviour of the alloyed powders and the phase structure of heat-treated samples were strongly dependent on milling duration. S. Sivakumar, In these study Aluminum matrix composites (AMCs) reinforced with hard metallic particles can be used as reinforcement to improve ductility. The present investigation focuses on using molybdenum (Mo) as potential reinforcement for Mo (0,6,12 and 18 vol.%) /6082Al AMCs. Mo particles were successfully retained in the aluminum matrix in its elemental form without any interfacial reaction. A homogenous distribution of Mo particles in the composite was achieved. The tensile test results showed that Mo particles improved the strength of the composite without compromising on ductility.

M. Zadra, et al. [13] This study introduces an alternative approach to the mechanical alloying of titanium, traditionally performed using fugitive process control agents (PCAs). In this work, calcium, magnesium, MgY, and CrY were employed as PCAs to effectively regulate the competing mechanisms of cold welding and particle fracture, thereby enhancing the overall process efficiency. The resulting at both low and high temperatures to optimize mechanical performance and microstructural quality. To further investigate the role of these PCAs, the sintered samples underwent high-temperature heat treatment.

Quan Yuan, et al. [14] Nanocrystalline Ti(C,N) powders were successfully synthesized via mechanical alloying (MA) using a blend of pure titanium, graphite, and titanium nitride. The study also explored the effect of adding nickel and molybdenum on the reaction kinetics. Phase evolution and powder morphology were characterized using X-ray diffraction (XRD) and transmission electron microscopy (TEM). The optimal synthesis conditions involved 20 hours of milling at a ball-to-powder weight ratio of 30:1 and a rotational speed of 400 rpm in a planetary ball mill.

The solid-state reaction proceeded in two distinct stages: initially, carbon atoms diffused into titanium, forming a Ti(C) supersaturated solid solution, which subsequently transformed into TiC. In the second stage, interdiffusion of C and Ni atoms led Ti(C,N) solid solution. The incorporation of 10 wt.% nickel or molybdenum significantly enhanced the reaction rate, with nickel demonstrating a more pronounced catalytic effect than molybdenum in accelerating the formation of nanostructured Ti(C,N) powders.

III. METHODOLOGY



IV. EXPERIMENTAL DETAILS

Mechanical Alloying

The process of mechanical alloying (MA) commences with the precise mixing of powders in specified proportions. Subsequently, the powder mixture is loaded into the mill together with the grinding medium, typically consisting of steel balls. The mixture is subsequently milled for a specified duration if a steady state is achieved, at which point the composition of each powder particle aligns with the proportions of the elements in the initial powder.

Planetary Ball Milling

Mechanical alloying was performed using the RETSCH PM100 (refer to Figure 4.2). This system enables several 100 grams of powder per batch. The term "planetary" derives from the unique motion of the milling vials, which are mounted on a rotating support disk. A specialized drive mechanism induces simultaneous rotation of vials nearby own axes while the disk itself rotates in the opposite direction.



Figure 1 Planetary Ball Mill.

This dual-motion setup generates complex centrifugal forces (illustrated in Figure 4.3), acting both from the vial rotation and the disk rotation. These forces subject the powder and grinding media inside the vials to intense mechanical interactions. As the vials and disk rotate counter to each other, the resulting forces alternate between synergistic and opposing directions. This dynamic causes the grinding balls to cascade along vial, producing frictional effects. Subsequently, the balls and powder are projected across the vial chamber, leading to high-energy collisions with the opposite wall—an impact-driven mechanism essential for effective particle refinement and alloy formation.

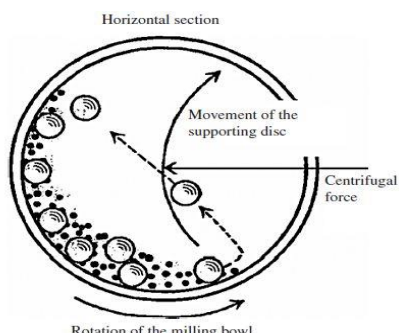


Figure: 2 Schematic view of motion of the ball and powder mixture.

In the older versions, it was not feasible to adjust the rotation rates of the disk and the vial independently; but, in the more recent versions, it is able to do so. Reliant on the extent of mill, there may be one, two, or even four milling stations. Figure 4.4 illustrates that grinding vials and balls can be made from a variety of materials, including zirconia, silicon nitride, chrome steel, agate, sintered corundum, WC, and Cr-Ni steel. These materials are available in a total of eight different varieties.

V. EXPERIMENTAL DETAILS

Experimental setup

In terms of weight percent, the material composition included Ti (60 gms) Mg (20 gms) and Fe (20 gms) powder. Consequently, one hundred grams of the material was extracted. Detailed below are the requirements and ball milling parameters.

Ball Milling Specifications	
Ball to Powder weight ratio	1:10
Milling media	Toluene
Speed	200 rpm
Ball material	Tungsten Carbide
Vial material	Tungsten Carbide
Container (vial) volume	250 ml
Utility volume	50-150 ml
Diameter of ball	10 mm
Weight of each ball	7.5 gms
Total weight of balls	750 gms
Total milling time	30 hrs.

The jar weight (vial), balls included and the powder with the milling media, toluene, all together was weighed 6.799 kg and the necessary counterweight in the PM100 were adjusted. The total milling time was 50hrs where in the samples were collected in every interval of 5hours.

X-Ray Diffraction.

Powdered material diffraction [19] is a key method for characterizing materials, giving structural information despite the fact the size of the crystals is small enough for single crystal x-ray diffraction methods. The use of powder diffraction has grown a lot of few years, throughout research and manufacturing. Since better instruments, data processing, and knowledge of what information can be gained. Powder diffraction makes it possible to quickly and non-destructively analyze mixtures with more than one component without having to prepare the samples in a lot of detail. This gives laboratories quickly analyze unknown materials and perform materials characterization in such fields as chemistry, materials science, geology, mineralogy, forensics, archaeology, and the biological and pharmaceutical sciences.

Powder Diffraction.

Perhaps the most used x-ray diffraction method for material characterization is powder XRD, which stands for X-ray diffraction. Powdered samples, as the name implies, often consist of microscopic grains of a single crystalline substance. Polycrystalline solids (large quantities of or film-like components) and particle suspensions in liquids are two more common areas of application for this method.

Scanning Electron Microscopy.

SEM, or scanning electron microscopy, is an effective tool for examining materials [20]. A scanning electron microscope is made up of a particle optical column, an empty system, electronic components and programs. The column is significantly shorter since the only lenses required are those located above the specimen, which focus the charged particles into a fine point on the object being studied surface. There are actually no lenses beneath the specimen. The specimen chamber, on the reverse hand, is larger since the SEM technique places no restrictions on the sample size other than those imposed by the specimen chamber. Users can acquire high magnification photos with a decent depth of field and examine specific crystals or other details. A high-resolution SEM scan can reveal information down to 25 Angstroms or greater. When used with the closely related technology of energy-dispersive microanalysis by X-rays (EDX, EDS, EDAX), the chemical structure of single crystals or features are able to calculate. Both scanning electron microscopy with microanalysis by X-rays strength be castoff in variation of ways to improve materials research.

A standard optical microscope has a maximum usable magnification of approximately 1000x. To improve resolution (and useful magnification), the wavelength that emits imaging radiation needs to be reduced. In electron microscopy, electrons are often accelerated to high energy ranging from 2 to 1000 keV (corresponding to wavelength of 0.027-0.0009 nm). There are numerous conceivable connections among the energetic electron & atoms of the object. If the specimen is incredibly tinny, electrons could permit through it unabsorbed and generate the image in a Transmission Electron Microscope. If the specimen gets thicker, electrons are no longer transported, leaving only particles (such as electrons, x-rays, and photons) emanating from the surface to provide information. This includes the signals generated by traditional SEMs.

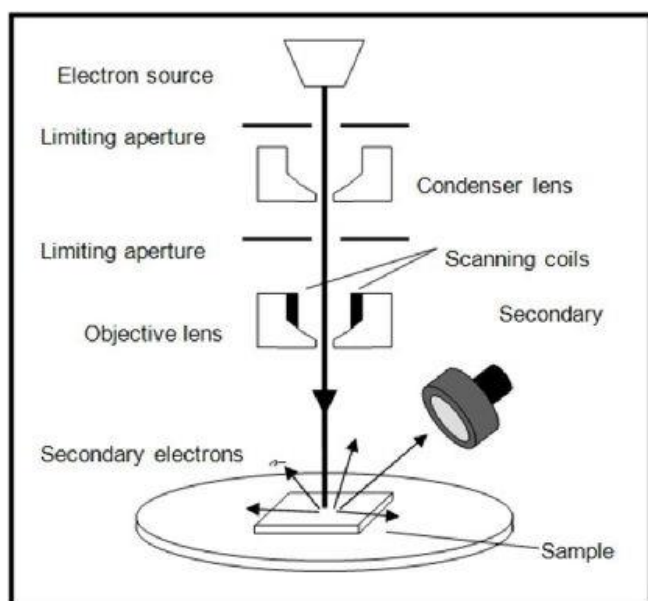


Figure 3 Schematic sketch of working principle of SEM.

Transmission Electron Microscopy.

Transmission Electron Microscopy (TEM) is a valuable morphological characterization method for nanomaterials [21]. Transmission electron microscopy (TEM) is a microscopy technique in which an electron beam is transmitted through an ultrathin object, reacting with it as it passes. The interaction of electrons sent through the material produces an image, which is magnified and focused onto an imaging device, which can be a fluorescent screen, a covering of photographic film, or a CCD camera sensor.

The TEM is built from the top down, with an emission source that can be either a tungsten filament or a lanthanum hexaboride (LaB6) source. For tungsten, this will take a shape of either a hairpin-style filament or a tiny spike-shaped filament. LaB6 sources use tiny single crystals. When connected to a high voltage source (usually ~100-300 kV), the cannon emits electrons into the vacuum through thermionic or field emission, depending on the current. Typically, a Wehnelt cylinder is used to help this extraction.

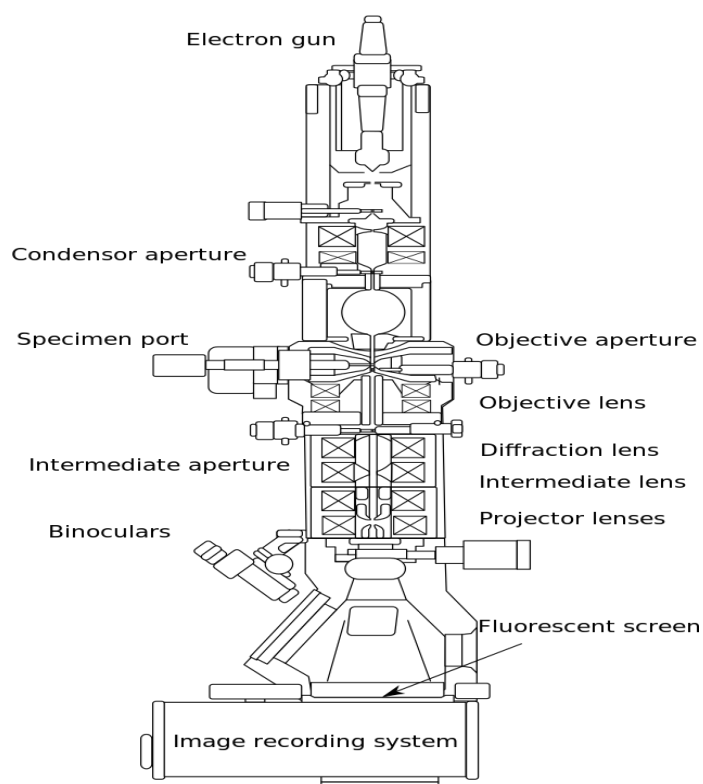


Figure 4. Transmission Electron Microscope.

Another effect of electrostatic fields is to constantly angle-deflect the electrons. Beam shifting in transmission electron microscopy (TEM) is achieved by coupling two directional deflections with a tiny intermediate gap.

VI. RESULTS AND DISCUSSION.

XRD study of ball milled powder.

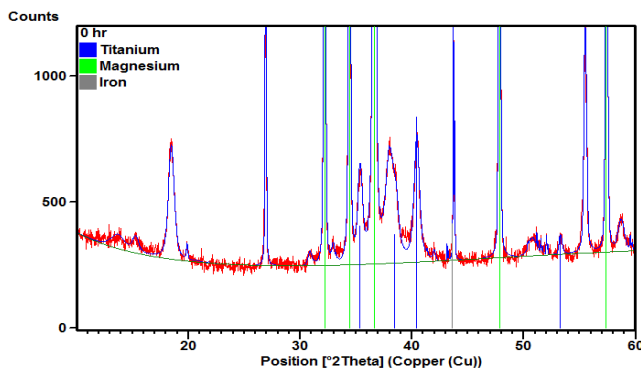


Figure 5. XRD for unmill powder sample.

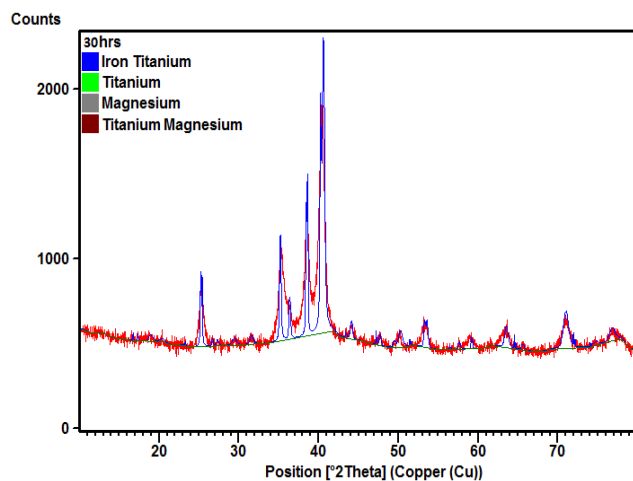


Figure 6. XRD of 30HR powder sample.

Milling duration progresses, say in the last part of 30 hours of milling time elemental peaks along with peaks of Solid solution are observed. Peaks of elemental phases then solid solution peaks have emerged. Such formation depends on atomic packing factor phenomenon; usually the atomic packing factor of BCC is comparatively lower than FCC lattice. Hence BCC solid solution is able to accommodate a greater number of atoms of different atomic radii. From the past research work it has been shown that diffusion of Mg normally promotes the formation of BCC solid solution rather than FCC. Hume-Rothery rules for solid solution formation in binary system depends on atomic size, valence electron, electron negativity and crystal structure of the elements involved. However, solid solution of multi component alloys containing three or more elements in high concentration is entirely a different phenomenon. Ternary component alloy of Ti, Mg and Fe enjoys the benefits of various elements that are added to strengthen its solid solution, especially those elements which possess different atomic radius compared to Ti. It is to be noted that the atomic radius of Ti is larger, while that of minor alloying elements. Crystal structure of Ti and Mg is HCP; Fe is BCC has multiple allotropic forms of crystal structure. Usually diffusion of elements with larger atomic radius into the crystal structure of solvent promotes the stabilization of BCC solid solution.

IJERTV14IS100072

(This work is licensed under a Creative Commons Attribution 4.0 International License.)

Scanning electron microscopy study of ball milled powders SEM image of unmilled powder samples. Unmilled powder samples consists Ti, Mg & Fe. Examining of unmilled powder displays circular like shape without any deformation. Figure 5.4 shows the revolution in the powder shape after 30 hour. Powders begin to deform and then agglomerate throughout ball milling process; partially flattened powder shape is observed during 30 hours of milling period as presented in figure 5.4. Such flattening happens owed to repetitive impinging of balls on the powder elements, these powder elements are sandwiched between the impinging balls and vial wall thus getting flattened. Welding and fracture of powder particle occurs in random directions. Hence, powders shape are begin to change. At extended milling time due to repeted joining and break powder particles begins to distingrate. If refining process is increased powders are formed flattened like shape shown in figure. Powder ball milled at 30 hour of ball milling shows extra levelling caused by layer by layer diffusion as a result of mechanical alloying mainly due to high impact (collision of balls).

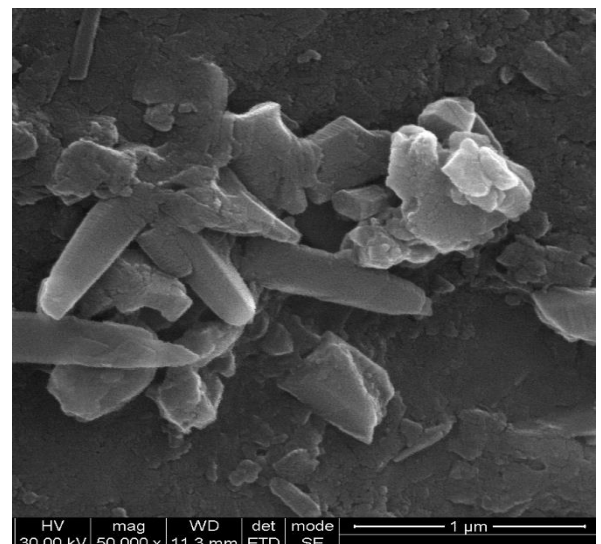


Figure 7. Micrograph for un mill powder sample.

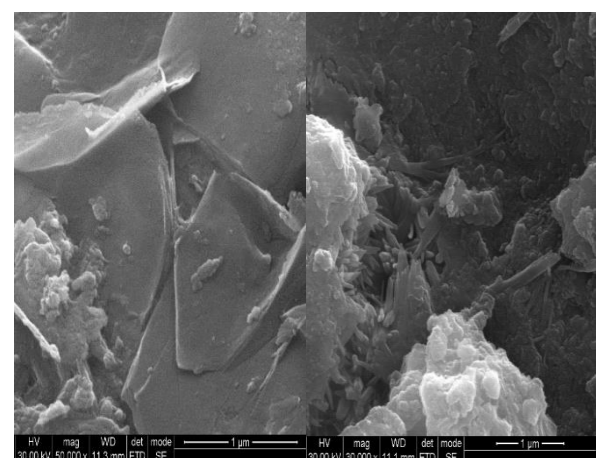


Figure 8. Micrograph for 30 hr milled powder sample
Transmission electron microscopy study of ball milled powders.

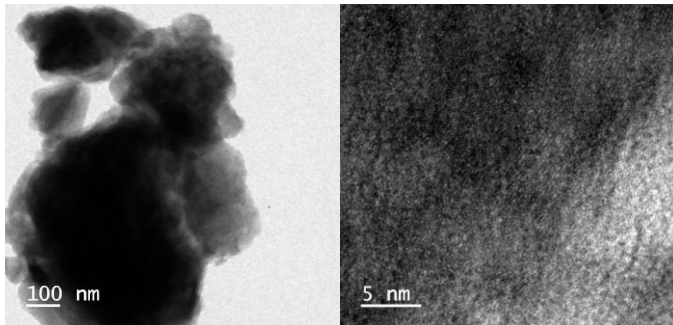


Figure 9 TEM micro graph for 30 hr milled powder sample.

Transmission electron microscopy (TEM) images (Fig. 5.5) indicate the diffusion of Mg and Fe in Ti lattice later 30 hours of time. Additionally, the XRD profile demonstrated that a Ti-rich solid solution had formed, as shown in Figure, with crystalline particles of Ti and Zr embedded in the Ti matrix. The XRD crystallite size determined using the Scherrer equation agrees with the TEM data, which show crystalline particles in the range of about 85 nm.

XRD Study of CIP CONSOLIDATED SINTERED COMPACT.

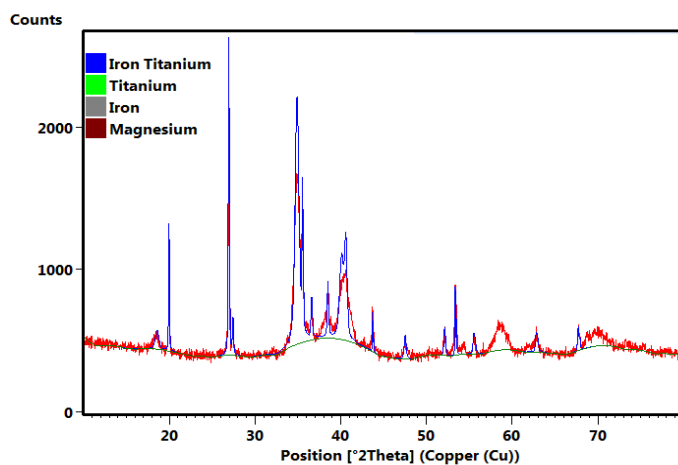


Figure 10. XRD graph for Solid sample.

SEM CHARACTERISATION OF CIP CONSOLIDATED SINTERED COMPACT

SEM image in Fig shows diffusion bonding obtained during microwave sintering, several phases can be seen, however porosities along with second phase particles are also observed.

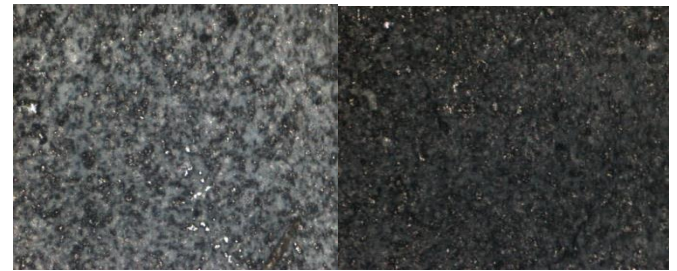


Figure 11 SEM micrograph of CIP consolidated and sintered (30 hours milling duration).

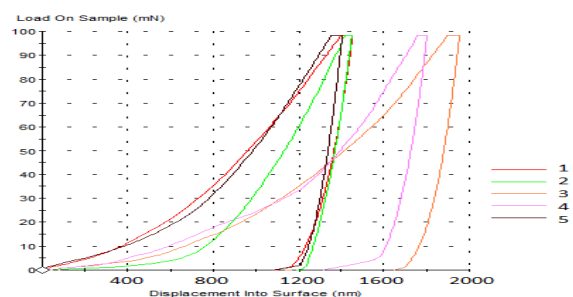
NANOINDENTATION

Solid solution strengthening causes higher nano hardness and elastic modulus in the CIP consolidated and sintered compacts. In addition, crystallization of amorphous phase and intermetallic compounds enhances the mechanical properties (nano hardness and elastic modulus). Nanoindentation load versus displacement curves show several discontinuities (pop in) resulting from elemental diffusion into solvent lattice and twinning during ball milling as well as CIP consolidation. Twinning is normally associated due to hcp structure of Mg. hcp structure has limited slip system compared to other cubic systems.

Table: Nanoindentation results of sintered CIP compacts.

Test	Modulus At Max Load GPa	Hardness At Max Load GPa	Load At Max Load mN
1	56.321	1.499	96.465
2	61.733	1.295	95.822
3	49.549	0.832	95.737
4	50.439	0.773	96.023
5	73.902	1.365	96.452
Average	58.388	1.152	96.099

Figure 12 Load versus displacement curve for Solid sample.



VII. DISCUSSIONS AND CONCLUSIONS.

The emphasis on material characterization has been shown in the respective results of the various analysis performed in the present investigation. The leading cause for XRD Bragg peak broadening is crystallite size refinement and an increase in the lattice strain.

The following inferences are drawn from the present investigation, which involves the synthesis of nanostructured Titanium-Magnesium-Iron alloy:

- The formation of Titanium-Magnesium and Titanium-Iron solid solutions is attributed to the ballistic diffusion of Mg and Fe atoms into the Ti lattice during mechanical alloying (MA), sustained over a 30-hour milling period.
- The observed shift in X-ray diffraction (XRD) peaks toward higher Bragg angles signifies the emergence of new phases. This peak displacement, coupled with the appearance of distinct diffraction signatures, confirms phase transformation induced by the alloying process.
- A marked reduction in peak intensity alongside pronounced peak broadening in the XRD pattern indicates a transition from a crystalline to an amorphous structure. This structural evolution is accompanied by significant grain refinement, with crystallite size reduced to approximately 34 nm after 30 hours of mechanical alloying.
- The morphology of milled powder shows more irregular in shape with the changes in the form of powders resulting from deformation seen by flattening and typical popcorn structure from the increase in the ball milling duration.
- Black dark spots in TEM SADP indicate nanocrystalline grains, and a smoky image shows amorphization. Agglomeration of particles and Nanocrystalline grains are prevalent. Thus, TEM results are consistent with XRD and SEM analysis.

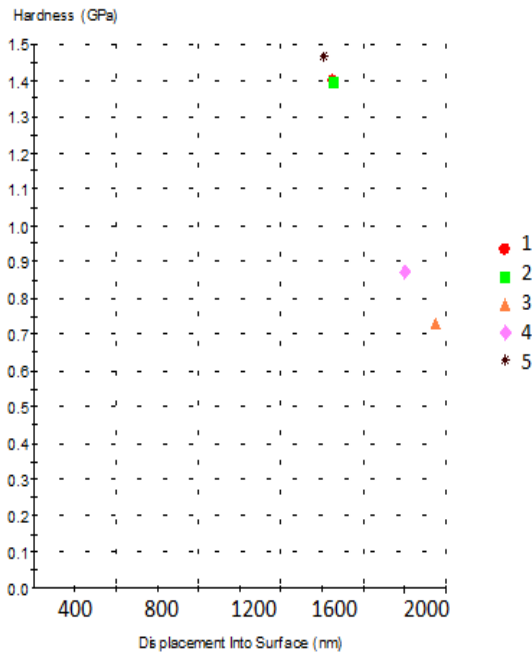


Figure 13 Hardness curve for Solid sample.

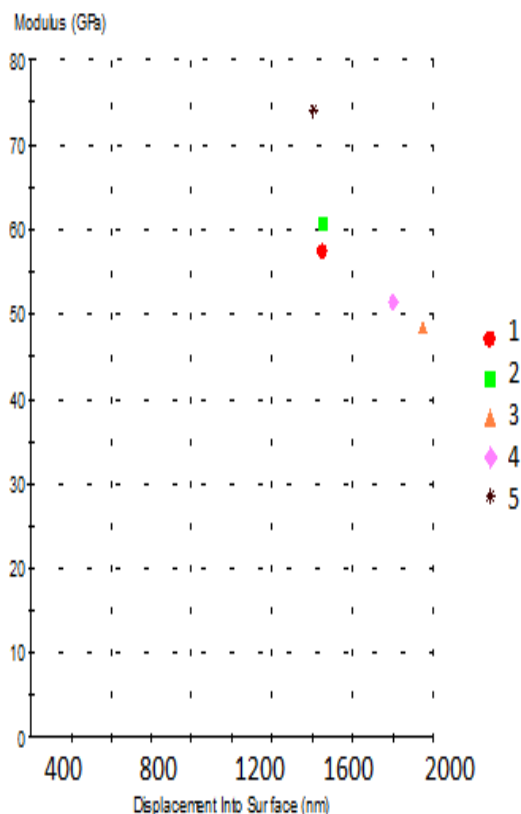


Figure 14 Modulus curve for Solid sample.

VIII. REFERENCES

- [1] Leyens, C.; Peters, M. Titanium and Titanium Alloys: Fundamentals and Applications; Wiley-VCH: Weinheim, Germany, 2003.
- [2] Mark T. Whittaker, Titanium Alloys, *Metals* 2015, 5, 1437-1439. doi:10.3390/met5031437.
- [3] Yassin Mustafa Ahmed, Khairul Salleh, Mohamed Sahari et. al. Titanium and its Alloy, International Journal of Science and Research, Volume 3 Issue 10, 2014, ISSN: 2319-7064.
- [4] Jitendra Sharan, Shantanu V. Lale, Veena Koul, Monu et.al, An Overview of Surface Modifications of Titanium and its Alloys for Biomedical Applications, Trends Biomater. Artif. Organs, 29(2), 176-187 (2015).
- [5] Horst E. Friedrich, Barry L. Mordike, Magnesium Technology Metallurgy, Design Data, Applications. Springer Berlin Heidelberg New York, ISBN-10 3-540-20599-3.
- [6] M. Avedesian, H. Baker, ASM Specialty Handbook: Magnesium and Magnesium Alloys, 1999.
- [7] S V Satya Prasad, S B Prasad, Kartikey Verma, The role and significance of Magnesium in modern day research-A review, Journal of Magnesium and Alloys, 2021, <https://doi.org/10.1016/j.jma.2021.05.012>.
- [8] G. Song, A. Atrens, Understanding magnesium corrosion—a frame- work for improved alloy performance, Adv. Eng. Mater. 5 (12) (2003) 837–858, <https://doi.org/10.1002/adem.200310405>.
- [9] G.L. Song, A. Atrens, Corrosion mechanisms of magnesium al- loys, Adv. Eng. Mater. 1 (1) (1999) 11–33, doi: 10.1002/(sici) 1527- 2648(199909)1:1 _ 11::aid- adem11 _ 3.0.co;2- n.
- [10] Jiangfeng Song, Jia She, Daolun Chen et. al, Latest research advances on magnesium and magnesium alloys worldwide, Journal of Magnesium and Alloys, 2020, 8, 1–41, <https://doi.org/10.1016/j.jma.2020.02.003>.
- [11] SC Gad, Strontium, Encyclopedia of Toxicology Elsevier, 2014, Volume 4, 405-406, <http://dx.doi.org/10.1016/B978-0-12-386454-3.00931-3>.
- [12] FatemehAlijani, RasoolAmini, et al., “Effect of milling time on the structure, micro-hardness, and thermal behavior of amorphous/nanocrystalline TiNiCu shape memory alloys developed by mechanical alloying”. Materials and Design 55 (2013) 373–380
- [13] M. Zadra. “Mechanical alloying of titanium” Materials Science & Engineering A583(2013)105–113
- [14] Quan Yuan, Yong Zheng, Haijun Yu “Synthesis of nanocrystalline Ti(C,N) powders by mechanical alloying and influence of alloying elements on the reaction” Int. Journal of Refractory Metals & Hard Materials 27 (2009) 121–125.
- [15] L.L. Meisnera, A.I. Lotkova, M.G. Ostapenko, E.Yu. Gudimovaa. “X-ray diffraction study of residual elastic stress and microstructure of near-surface layers in nickel-titanium alloy irradiated with low-energy high-current electron beams” Applied Surface Science 280 (2013) 398– 404
- [16] P. Majumdar, S.B. Singh, M. Chakraborty. “Elastic modulus of biomedical titanium alloys by nano-indentation and ultrasonic techniques—A comparative study” Materials Science and Engineering A 489 (2008) 419– 425
- [17] D.D. Radev. “Mechanical synthesis of nanostructured titanium–nickel alloys” Advanced Powder Technology 21 (2010) 477–482
- [18] Chul-Jin Choi. “Preparation of ultrafine TiC-Ni cermet powders by mechanical alloying” Journal of Materials Processing Technology 104 (2000) 127-132